SCIENTIFIC REPORTS

OPEN

SUBJECT AREAS:
NANOPARTICLES
IMAGING TECHNIQUES AND AGENTS

Received
4 March 2014

Accepted
29 April 2014

Published
16 May 2014

Correspondence and requests for materials should be addressed to J.-I.C. (jichao@faculty.nctu.edu.tw)

Labeling of neuronal differentiation and neuron cells with biocompatible fluorescent nanodiamonds

Tzu-Chia Hsu[1], Kuang-Kai Liu[2], Huan-Cheng Chang[3], Eric Hwang[1,2,4] & Jui-I Chao[1,2]

[1]Institute of Molecular Medicine and Bioengineering, National Chiao Tung University, Hsinchu 30068, Taiwan, [2]Department of Biological Science and Technology, National Chiao Tung University, Hsinchu 30068, Taiwan, [3]Institute of Atomic and Molecular Sciences, Academia Sinica, Taipei 10617, Taiwan, [4]Institute of Bioinformatics and Systems Biology, National Chiao Tung University, Hsinchu 30068, Taiwan.

Nanodiamond is a promising carbon nanomaterial developed for biomedical applications. Here, we show fluorescent nanodiamond (FND) with the biocompatible properties that can be used for the labeling and tracking of neuronal differentiation and neuron cells derived from embryonal carcinoma stem (ECS) cells. The fluorescence intensities of FNDs were increased by treatment with FNDs in both the mouse P19 and human NT2/D1 ECS cells. FNDs were taken into ECS cells; however, FNDs did not alter the cellular morphology and growth ability. Moreover, FNDs did not change the protein expression of stem cell marker SSEA-1 of ECS cells. The neuronal differentiation of ECS cells could be induced by retinoic acid (RA). Interestingly, FNDs did not affect on the morphological alteration, cytotoxicity and apoptosis during the neuronal differentiation. Besides, FNDs did not alter the cell viability and the expression of neuron-specific marker β-III-tubulin in these differentiated neuron cells. The existence of FNDs in the neuron cells can be identified by confocal microscopy and flow cytometry. Together, FND is a biocompatible and readily detectable nanomaterial for the labeling and tracking of neuronal differentiation process and neuron cells from stem cells.

Stem cells are unspecilized cells that have two general characteristics, including self-renew to produce more stem cells and differentiate to specialized cell types[1,2]. Embryonic stem (ES) cells are pluripotent cells derived from inner mass of blastocytes[3,4]. ES cells express specific stem cell markers of transcription factors, such as Oct-4, Sox2 and NANOG[5–8]. Somatic cells can be induced back to pluripotency by the stimulation of transcription factors, Oct3/4, Sox2, c-Myc, and Klf4, that called induced pluripotent stem (iPS) cells[9,10]. Moreover, stem cells also express other stem cell markers on the cell surface, such as stage-specific embryonic antigen (SSEA)-1 in mouse[11] and SSEA-4 in human[12]. Embryonal carcinoma stem (ECS) cells are considered to be the malignant counterparts of ES cells[4,8,13]. ECS cells were similar to ES cells in morphology, marker expression and growth behavior[8,13]. These stem cells were derived from teratocarcinoma that could alter the phenotype from the malignant to non-malignant after differentiation[4,14–16]. The ES, iPS and ECS cells are pluripotent and can be differentiated into a variety of cell types.

Stem cells provide an opportunity for therapeutics to cure neurological disorders or injuries, such as Parkinson's and Alzheimer's diseases[17–20]. Parkinson's disease is resulted from the loss of dopaminergic neurons in the substantia nigra[18,21]. Stem cells express glial-cell-line-derived neurotrophic factor, which has been shown to improve the survival and function of dopaminergic neurons that may be one approach to stop the death of dopaminergic neurons[20,22]. Furthermore, stem cells can generate cholinergic neurons to improve the cognitive function of Alzheimer's disease patients[18,19].

Nanodiamond (ND) is a promising carbon-based nanomaterial for biomedical applications[23–31]. NDs have several advantages, including physical and chemical properties, biocompatibility, and optical stability. NDs can emit fluorescence without photobleaching[24–26]. More importantly, NDs did not induce considerable toxicity in various cells[24,27,32–37]. The histopathological examination shows that there are no adverse reactions after injection with NDs in mice and rats[38]. Furthermore, intravenously administered high dosage of NDs did not induce substantial liver and systemic toxicity[39]. NDs are currently developing for the labeling of stem cells or progenitor cells[33,36,40,41]. However, the applications of NDs on the neuronal differentiation and the neuron cells are still unclear.

a

Cell lines	Species	Stem cell types	Culture medium
P19	Mouse	Pluripotent embryonal carcinoma	MEM
NT2/D1	Human	Pluripotent embryonal carcinoma	DMEM

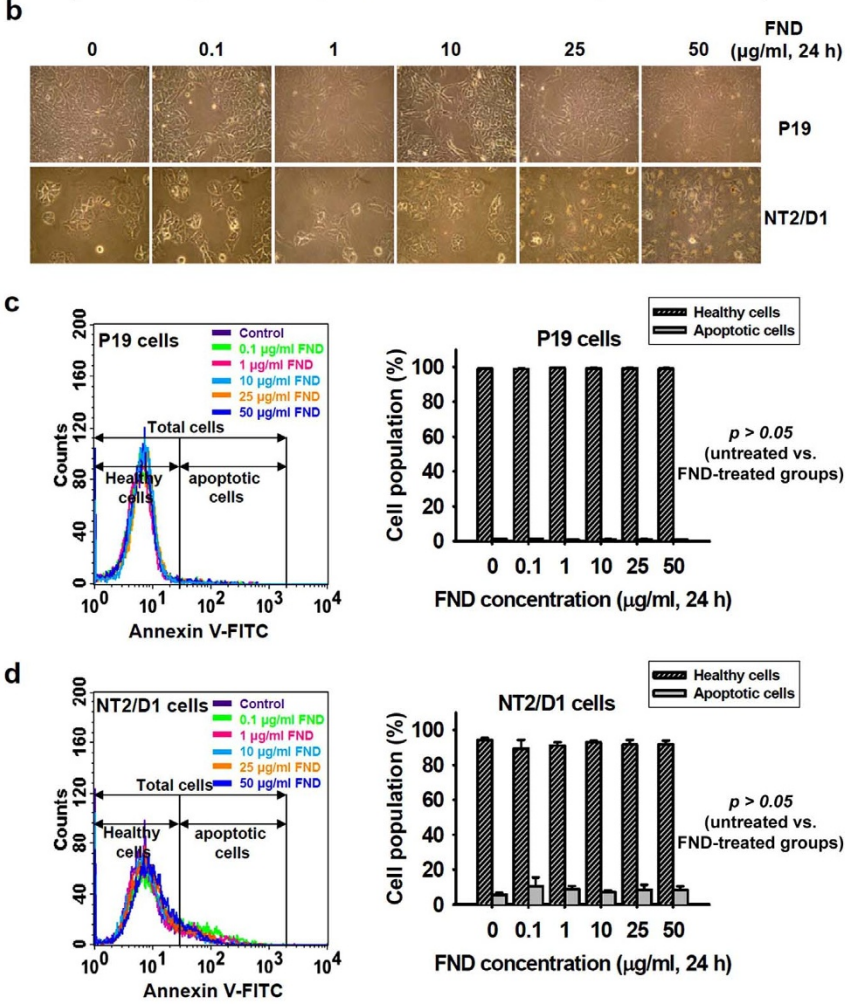

Figure 1 | FNDs do not affect cell morphology, viability and apoptosis in the ECS cells. (a) Two pluripotent embryonic carcinoma stem (ECS) cell lines, P19 and NT2/D1, were used in this study. (b) P19 and NT2/D1 cells were plated at a density of 7×10^5 cells or 4×10^5 cells per 60-mm Petri dish, respectively. Then the cells were treated with or without FND (0.1–50 μg/ml for 24 h). Representative phase-contrast photomicrographs (200× magnification) show the cell morphology of P19 and NT2/D1 cells. (c) P19 cells were plated at a density of 7×10^5 cells per 60-mm Petri dish. (d) NT2/D1 cells were plated at a density of 4×10^5 cells per 60-mm Petri dish. Then the cells were treated with or without FNDs (0.1–50 μg/ml for 24 h). At the end of treatment, the levels of apoptotic cells were determined by Annexin V-FITC staining and analyzed by flow cytometer. The Annexin V^+ cells represented cells undergoing apoptosis. The populations of healthy and apoptotic cells were quantified from a minimum of 10,000 cells using CellQuest software. Results were obtained from three separate experiments and the bar represented the mean ± S.E. The percentages of healthy and apoptotic cell populations were not significantly altered by treatment FNDs in both P19 and NT2/D1 cells ($p > 0.05$).

The effects of NDs on the neuronal differentiation and potential applications derived from stem cells were previously undetermined. In this study, we provide the cytotoxic evaluations and labeling applications in the neuronal differentiation and neuron cells from ECS cells using fluorescent nanodiamond (FND). ECS cells can be maintained as undifferentiated cells that provide convenient tools in studying the differentiation process and function of stem cells. FND particles can be used for the labeling and tracking of neuronal differentiation and neuron cells, which may allow developing potential therapeutics for neurological disorders or injuries.

Results

FND does not alter the cytotoxicity, cell growth ability and apoptosis in the ECS cells. The ECS cell lines, including P19 and NT2/D1, were investigated on the biocompatibility and neuronal differentiation following treatment with FNDs (Figure 1a). The P19 cells were derived from mouse ECS cells, which were cultured in MEM medium, and the NT2/D1 cells were derived from human ECS cells, which were cultured in DMEM medium (Figure 1a). These cells were treated with or without FNDs (0.1–50 μg/ml for 24 h). The cell growth and number of P19 and NT2/D1 cells after treatment with FNDs were similar to the untreated cells (Figure 1b). Subsequently, the apoptotic effect was investigated following FND treatment in ECS cells by Annexin V-FITC staining. The fluorescence intensities of Annexin V-FITC (indicating apoptotic cells) were not significantly increased by treatment with FNDs (0.1–50 μg/ml for 24 h) in both P19 and NT2/D1 cells (Figure 1c and 1d, $p > 0.05$). These data also verified that FND did not alter on the percentage of population of healthy cells (Figure 1c and 1d, $p > 0.05$). To further examine the effect of FNDs on the cell growth

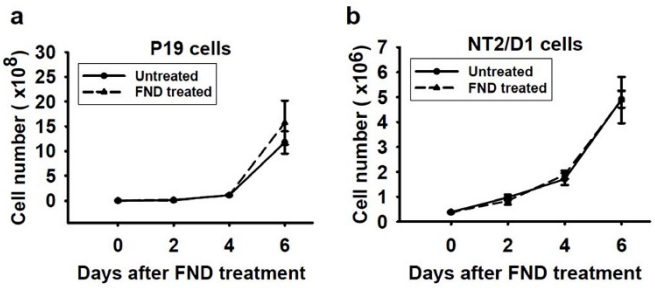

Figure 2 | FNDs do not inhibit the growth ability of ECS cells. (a) P19 cells or (b) NT2/D1 cells were plated at a density of 1×10^6 cells per 100-mm Petri dish for 16–20 h. Then the cells were treated with or without FNDs (50 μg/ml for 24 h). For counting the total cell number, the cells were re-cultured in fresh medium by every 2 d until total 6 d. Results were obtained from three separate experiments and the bar represented the mean ± S.E. The cell numbers were not significantly altered by treatment with FNDs in both P19 and NT2/D1 cells ($p > 0.05$).

ability, P19 and NT2/D1 cells were treated with or without 50 μg/ml FNDs for 24 h and then re-cultured for 6 days. The total cell number was counted every 2 days until day 6. P19 cells displayed relative higher cell growth rate than NT2/D1 cells; however, FNDs did not significantly alter the cell growth ability in either P19 or NT2/D1 cells (Figures 2a and 2b, $p > 0.05$).

Detection and uptake ability of FND in ECS cells. To determine the uptake ability of FNDs in ECS cells, the cells were treated with or without FNDs (0.1–50 μg/ml) for 24 h and the fluorescence intensities of FNDs in cells were analyzed by flow cytometry. The fluorescence intensities of FNDs were increased via a concentration-dependent manner in both P19 and NT2/D1 cells following treatment with FNDs (Figure 3a and 3b). The ESC cells were characterized by a stem marker protein SSEA-1, which was recognized by incubated with mouse anti-SSEA-1 antibody and then stained with goat anti-mouse IgG Cy3 antibody (Figure 4a). Moreover, the presence of FNDs in cells was observed by confocal microscope. The red fluorescence of FNDs was detected mainly in the cytoplasm (Figure 4a, the arrows). In addition, the protein levels of SSEA-1 following treatment with FNDs were analyzed by Western blot (Figure 4b). Treatment with FNDs (50 μg/ml for 24 h) did not significantly alter the protein expression of SSEA-1 in the ESC cells ($p > 0.05$).

Neuronal differentiation of ECS cells by retinoic acid induction. The images of differentiated neuron cells were observed by phase contrast or confocal microscopy. ECS cells were formed embryoid bodies by treatment with RA under phase contrast microscope observation (Supplementary Figure S1a, red arrows). After ECS cells were terminally differentiated, numerous neurites can be observed to sprout from the cell bodies (Supplementary Figure S1a, black arrows). Moreover, the P19 ECS cells and differentiated neuron cells were incubated with mouse anti-SSEA-1 and rabbit

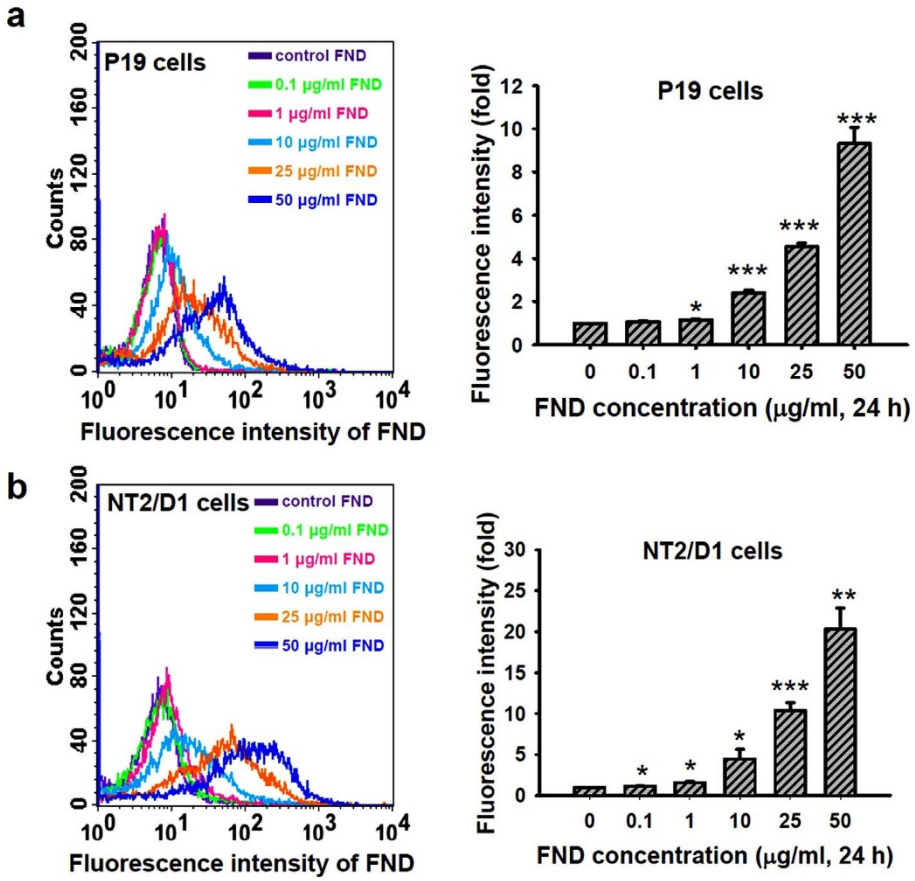

Figure 3 | The uptake ability of FNDs in the ECS cells by flow cytometry. (a) P19 cells were plated at a density of 7×10^5 cells per 60-mm Petri dish. (b) NT2/D1 cells were plated at a density of 4×10^5 cells per 60-mm Petri dish. Then the cells were treated with or without FNDs (0.1–50 μg/ml for 24 h). At the end of treatment, the cells were trypsinized and then subjected to flow cytometer. The fluorescence intensity of FNDs was excited with wavelength 488 nm, and the emission was collected with > 650 nm signal range (FL3-H). The fluorescence intensity of FNDs was quantified from a minimum of 10,000 cells by CellQuest software. Results were obtained from three separate experiments and the bar represented the mean ± S.E. $^*p < 0.05$, $^{**}p < 0.01$ and $^{***}p < 0.001$ indicate significant difference between control and FND treatment.

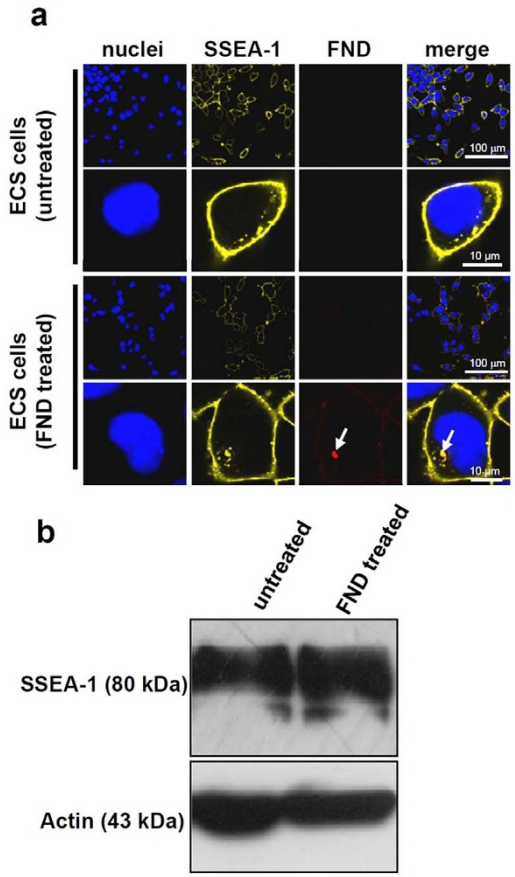

Figure 4 | The detection and location of FNDs in the ECS cells. (a) P19 cells were plated a density of at 7×10^5 cells per 60-mm Petri dish for 16–20 h. Then the cells were treated with or without FNDs (50 μg/ml for 24 h). At the end of treatment, the cells were incubated with mouse anti-SSEA-1 antibody and then stained with goat anti-mouse IgG Cy3 antibody. The nuclei were stained with Hoechst 33258. The fluorescence intensity of FNDs was excited with wavelength 580 nm, and the emission was collected in 600-700 nm. The fluorescence intensity of nuclei was excited with 405 nm and the emission was collected in 415–485 nm. The fluorescence intensity of SSEA-1 was excited with 543 nm, and the emission was collected in 560–580 nm. The nuclei display blue color. SSEA-1 displays yellow color. FND displays red fluorescence. The arrows indicate the location of FND in cytoplasm. (b) P19 cells were plated at a density of 7×10^5 cells per 60-mm Petri dish for 16–20 h. Then the cells were treated with or without FNDs (50 μg/ml for 24 h). At the end of treatment, the total proteins of cell extracts were collected and subjected to Western blot analysis using specific anti-SSEA-1 and anti-actin antibodies. Actin was a loading control. The representative Western blot data were shown from one of three separate experiments with similar findings.

anti-β-III-tubulin (TUJ1) antibodies, and then incubated with goat anti-mouse IgG Cy3 and goat anti-rabbit HiLyte Fluor 488 antibodies. Supplementary Figure S1b shows that P19 ECS cells displayed the red color of SSEA-1 proteins. In contrast, the differentiated neuron cells displayed the green color of β-III-tubulin.

Labeling and tracking of neuronal differentiation in ECS cells by FND. Figure 5a shows a model that the ECS and differentiated neuron cells were labeled with FNDs. To detect the fluorescence intensities of FNDs during neuronal differentiation, P19 cells were treated with FNDs (50 μg/ml for 24 h) and then the cells were differentiated into neuron cells by RA induction. The fluorescence intensities of FNDs increased in both the undifferentiated and differentiated neuron cells following FND treatment (Figure 5b). After quantification, the fluorescence intensities of FNDs in the undifferentiated cells and differentiated neuron cells were higher than the FND-untreated cells ($p < 0.05$). To further determine the location and distribution of FND particles in the differentiated neuron cells, the undifferentiated P19 cells were treated with FNDs (50 μg/ml for 24 h) and then differentiated into neuron cells by RA induction. The cellular morphology of P19 and differentiated neuron cells with FND treatment were observed under a phase contrast microscope (Figure 5c). The FND-treated P19 cells can be readily differentiated into neuron cells by RA treatment (Figure 5d). FND particles were observed in the cytoplasm of undifferentiated ECS and differentiated neuron cells (Figure 5d). FNDs remained in the cytoplasm of differentiated neuron cells even after long-term culturing for 7 days (Figure 5d).

FND does not alter the gene and protein expressions of neuron marker β-III-tubulin in neuronal differentiation. The gene expression of neuron marker β-III-tubulin was analyzed by reverse transcription-polymerase chain reaction (RT-PCR). The PCR products of β-III-tubulin and actin were 749 and 556 bps, respectively (Figure 6a). Actin was used as an internal control, which expressed in both the undifferentiated and differentiated cells. The mRNA levels of β-III-tubulin were significantly increased when P19 cells were differentiated into neuron cells (Figure 6b, $p < 0.05$). However, treatment with FNDs did not significantly affect the mRNA levels of β-III-tubulin during the neuronal differentiation (Figure 6c, $p > 0.05$). Moreover, the protein levels of β-III-tubulin were increased when P19 cells differentiated into neuron cells (Figure 6c and 6d). However, the fluorescence intensities of β-III-tubulin were not significant alteration by FND during the neuronal differentiation (Figure 6d, $p > 0.05$).

FND does not induce cytotoxicity and apoptosis during neuronal differentiation in ECS cells. To examine the cytotoxicity of FNDs on the neuronal differentiation of ECS cells, P19 cells were differentiated into the neuron cells and analyzed by MTT assays. Figure 7a shows that FNDs did not significantly reduce the cell viability in the differentiated neuron cells ($p > 0.05$). In addition, Annexin V-FITC staining was used to examine the apoptotic effect of FNDs in the neuronal differentiation. The fluorescence intensities of Annexin V-FITC were not significantly altered by treatment with FNDs (50 μg/ml for 24 h) during neuronal differentiation (Figure 7b and 7c, $p > 0.05$). These data also verified that FND did not significantly alter on the percentage of healthy cell population ($p > 0.05$).

Labeling and tracking of neuron cells by FND. Figure 8a shows a model that the neuron cells differentiated from ECS cells were labeled with FND. To determine the fluorescence intensities and uptake ability of FNDs in the differentiated neuron cells, the neuron cells derived from P19 cells were treated with or without FNDs (50 μg/ml for 24 h) and analyzed by flow cytometry. The fluorescence intensities of FND increased in both the P19 ECS cells and differentiated neuron cells (Figure 8b). After quantification, the fluorescence intensities of FNDs in both P19 ECS and neuron cells were higher than the FND-untreated cells (Figure 8c). However, the fluorescence intensity (uptake ability) of FNDs in the undifferentiated ECS cells was around 7-folds higher than the neuron cells (Figure 8c). To further investigate the location and distribution of FND in the neuron cells, the differentiated neuron cells were analyzed by confocal microscopy. The images showed that FNDs were located in the cell surface or were taken into the neuron cells (Figure 8d).

FND does not induce cytotoxicity and apoptosis in neuron cells. To examine cytotoxicity following treatment with FNDs in neuron cells, the differentiated neuron cells were treated with or without FNDs (50 μg/ml for 24 h) and analyzed by MTT assay. FNDs did

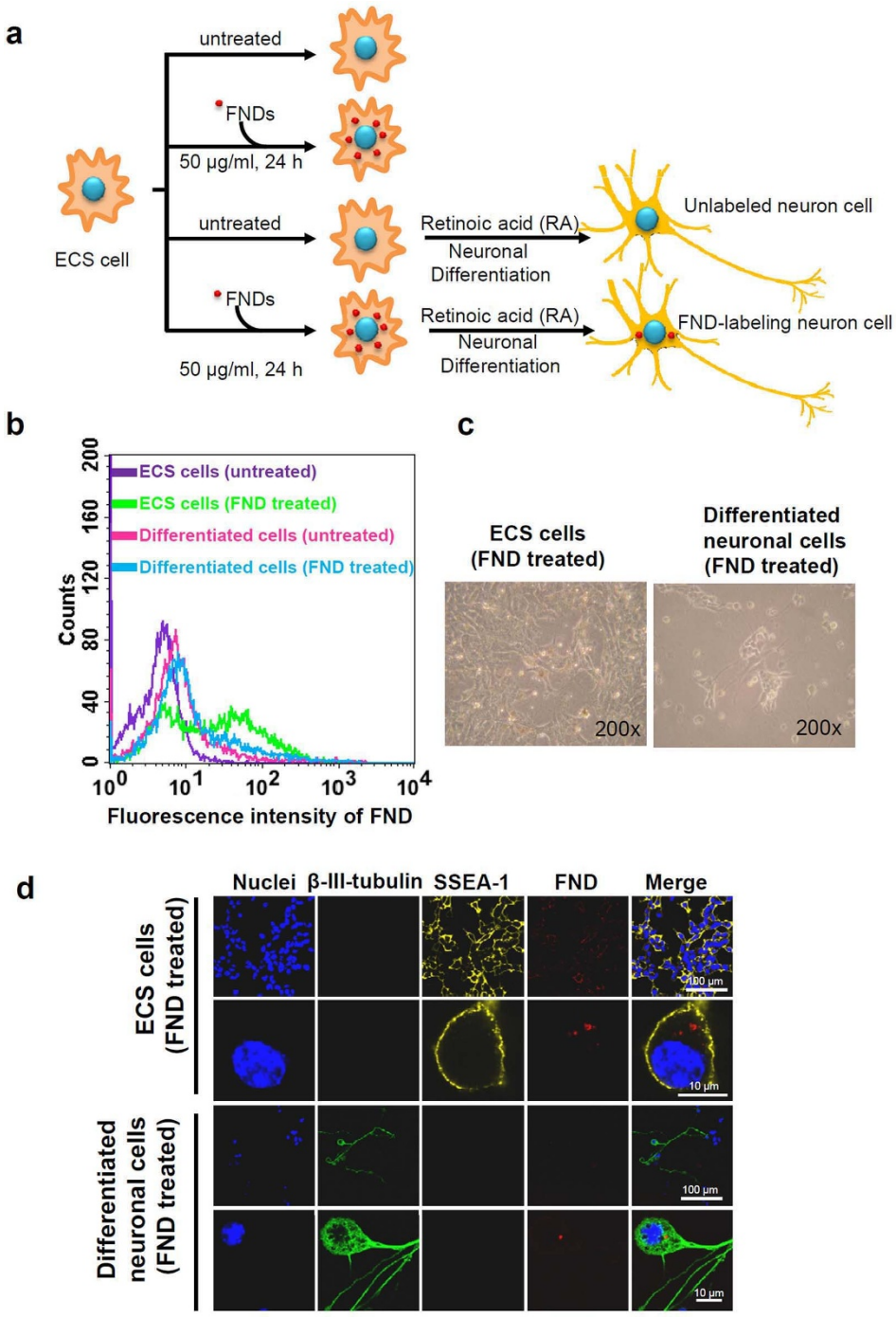

Figure 5 | The labeling and tracking of neuronal differentiation of ECS cells using FNDs. (a) A model of ECS and neuronal differentiation labeled with FND. (b) P19 cells were treated with or without FNDs (50 μg/ml for 24 h). Then the cells were differentiated into neuron cells by RA induction. The fluorescence intensity of FND in P19 and the differentiated neuron cells were measured by flow cytometer. The fluorescence intensity of FND was excited with wavelength 488 nm, and the emission was collected by >650 nm signal range (FL3-H). (c) P19 cells were treated with 50 μg/ml FNDs for 24 h. Then the cells were differentiated into neuron cells by RA induction. The cell morphology of P19 cells and differentiated neuron cells were observed under a phase contrast microscope. (d) The P19 cells and differentiated neuron cells were incubated with mouse anti-SSEA-1 and rabbit anti-β-III-tubulin antibodies, and then incubated with goat anti-mouse IgG Cy3 and goat anti-rabbit IgG HiLyte Fluor 488 antibodies. The nuclei were incubated with Hoechst 33258. The red fluorescence intensity of FND was excited with wavelength 580 nm, and the emission was collected in 600–700 nm. The fluorescence intensity of nuclei was excited with 405 nm and the emission was collected in 415–485 nm. The fluorescence intensity of β-III-tubulin was excited with 488 nm, and the emission was collected in 505–545 nm. The fluorescence intensity of SSEA-1 was excited with 543 nm, and the emission was collected in 560–580 nm. The nuclei display blue color. The SSEA-1 is indicated as yellow color. The β-III-tubulin shows green color.

not markedly reduce cell viability in neuron cells (Figure 9a, $p > 0.05$). In addition, Annexin V-FITC staining was used to examine the apoptotic levels following treatment with FNDs in these differentiated neuron cells. The fluorescence intensities of Annexin V-FITC were not altered by treatment with FNDs (50 μg/ml for 24 h) in neuron cells (Figure 9b and 9c). After quantification, the percentages of healthy and apoptotic cell populations were not significantly altered by FNDs (Figure 9c, $p > 0.05$).

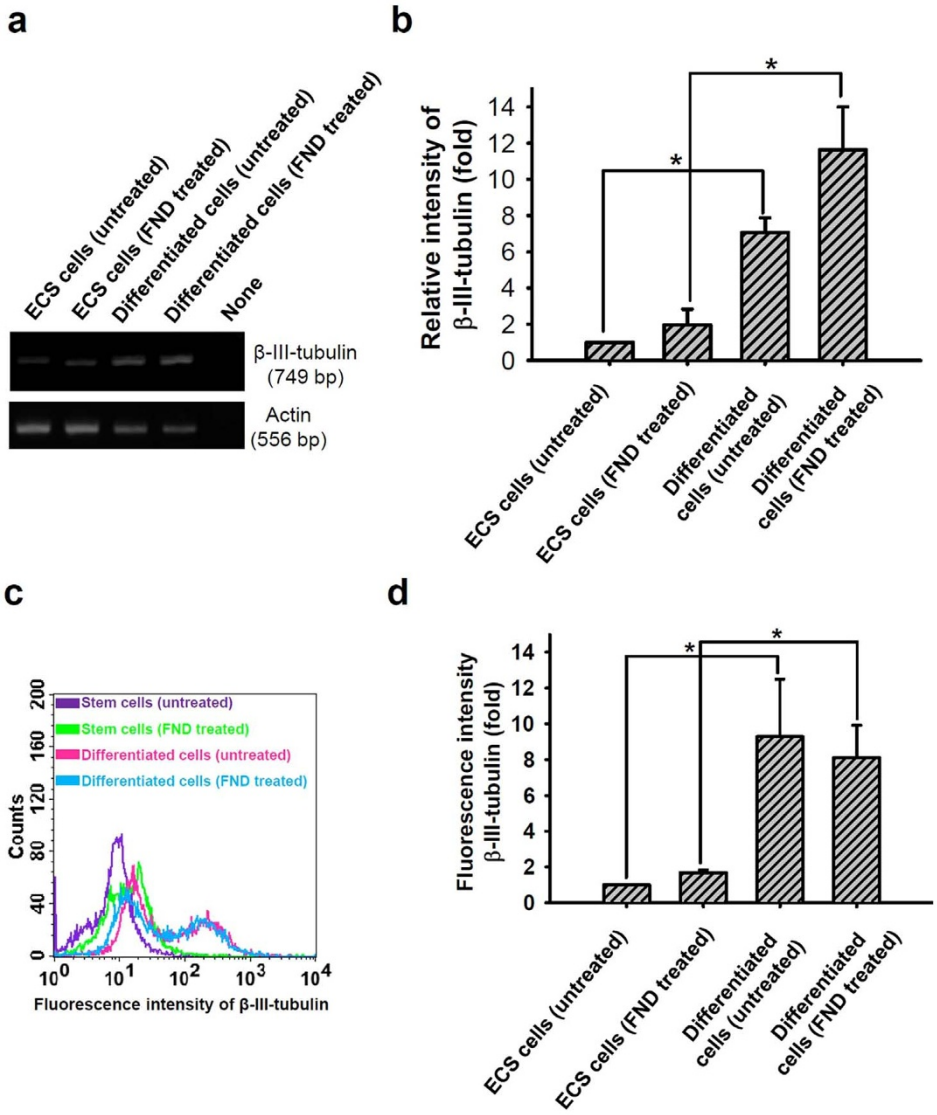

Figure 6 | FNDs do not alter the gene and protein expressions of β-III-tubulin during neuronal differentiation. (a) P19 ECS cells were treated with or without FNDs (50 μg/ml for 24 h), and then the cells were differentiated into neuron cells by RA induction. Total cellular RNA was purified for reverse transcription-polymerase chain reaction (RT-PCR) analysis. The RT-PCR amplified gene products of β-III-tubulin and actin were 749 and 556 bps, respectively. Actin is an internal control gene. (b) The mRNA levels were analyzed by semi-quantification. Results were obtained from three separate experiments and the bar represented the mean ± S.E. $*p < 0.05$ indicates significant difference between the ECS cells and differentiated cells following treatment with or without FND. (c) P19 cells were treated with or without 50 μg/ml FNDs for 24 h. P19 or differentiated neuron cells were incubated with anti-β-III-tubulin antibody, and then incubated with goat anti-rabbit IgG HiLyte Fluor 488 antibody. The fluorescence intensity of β-III-tubulin in P19 cells and differentiated neuron cells were analyzed by flow cytometer. (d) The fluorescence intensity was quantified from a minimum of 10,000 cells by CellQuest software. Results were obtained from four separate experiments and the bar represents the mean ± S.E. $*p < 0.05$ indicates significant difference between the ECS cells and differentiated cells following treatment with or without FND.

Discussion

The ECS cells provide a stem cell system for investigating neuronal differentiation process[14–16]. Both P19 and NT2/D1 ECS cells are pluripotent that can be differentiated into the neuronal lineages by RA induction[14–16]. We found that the fluorescence intensities of FNDs were increased in both the mouse P19 and human NT2/D1 ECS cells by treatment with FNDs. The findings show that FND particles can be taken into ECS cells; however, FNDs did not affect the cellular physiological functions, including cellular morphology, viability, growth ability, and stem cell marker protein expression. Furthermore, FNDs did not alter the neuron marker β-III-tubulin expression during the neuronal differentiation. Interestingly, the existence of FND particles in the neuron cells did not induce cytotoxicity and apoptosis. This study demonstrates that FND is a biocompatible and detectable nanomaterial during the process of neuronal differentiation and in the differentiated neuron cells from ECS cells. Various strategies of stem cell therapy are currently being developed, including ES and iPS cells. ES and iPS cells are pluripotent that can be differentiated into neural cells[42]. Thus, FND may be applied as a labeling agent for the neuronal differentiation of ES and iPS cells.

RA is a vitamin A derivative converted from retinol. ECS cells can be developed into neuron cells by RA induction[14,43]. After RA treatment, the ECS cells will aggregate to form embryoid bodies[43]. We found that embryoid bodies were aggregates in the RA-treated ECS cells and further generated neuronal lineages. During neuritogenesis, the neurites were growth from the differentiated neuronal lineages. RA enters nucleus of cells via cellular RA-binding protein (CRABP),

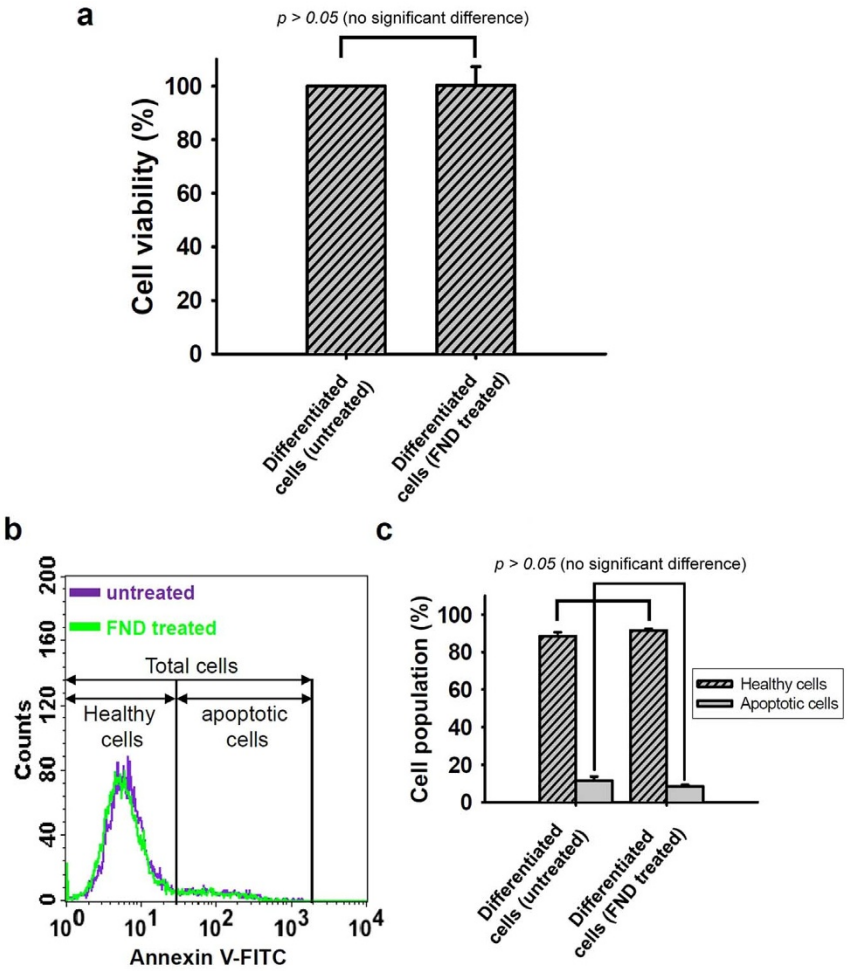

Figure 7 | FNDs do not induce cytotoxicity and apoptosis in the neuronal differentiation of ECS cells. (a) P19 cells were treated with FNDs (50 μg/ml for 24 h), and then differentiated into neuron cells. The differentiated cells were plated at a density of 7×10^4 cells per well in 24-well plate, and the cell viability was measured by MTT assays. Results were obtained from three separate experiments and the bar represented the mean ± S.E. (b) P19 ECS cells were treated with FNDs (50 μg/ml for 24 h), and then differentiated into neuron cells. The differentiated cells were collected for flow cytometer analysis. The effect of apoptosis was determined by Annexin V-FITC staining using flow cytometer analysis. The populations of Annexin V^+ cells represented cells undergoing apoptosis. (c) The populations of healthy and apoptotic cells were quantified from a minimum of 10,000 cells using CellQuest software. Results were obtained from three separate experiments and the bar represented the mean ± S.E. The percentages of healthy and apoptotic cell populations were not significantly altered by treatment with FNDs ($p > 0.05$).

and then interacts with members of hormone receptor superfamily such as the RA receptor (RAR) and retinoid X receptor (RXR)[44]. The above complex will interact with retinoic acid response element (RARE) to activate the differentiation gene expression[44]. There are several specific markers to identify whether the cells are neuronal lineages, including neuron-specific class III β-tubulin[45]. The mRNA and protein levels of β-III-tubulin were increased when ECS cells differentiated into neuron cells. However, the existence of FNDs in the RA-induced differentiated neuron cells did not alter both the gene and protein expressions of β-III-tubulin.

Stem cells are developing for therapeutics of neural injuries and neurodegenerative diseases[17–20]. Nanomaterials are developing for improving the efficiency of neuronal differentiation by RA delivery. For example, RA-loaded PEI was formed by electrostatic interactions[46]. RA released from nanoparticles could interact with RA receptor in inducing neuronal differentiation[46,47]. The ND's surface provides a unique platform for the conjugation of drugs or biomolecules[27–29]. In addition to bio-imaging and -labeling, NDs may be developed for drug delivery using in the neuronal differentiation of stem cells.

NDs did not disturb the physiological functions on the adipogenic and osteogenic differentiations[33,36]. The existence of ND particles did not alter the mRNA levels of PPARγ (a lipid-activated transcription factor which promotes the adipogenesis) and adiponectin (an adipocyte marker)[33]. Moreover, the existence of NDs in the mesenchymal stem cells has no obvious side effects in the osteogenic differentiation[40]. Recently, the ND-labeled lung progenitor cells can be preferentially reside at terminal bronchioles of the lungs after intravenous transplantation, which provide potential therapy of lung injury[41]. FNDs did not disturb the protein expression of SSEA-1 in ECS cells. We also found that FNDs were co-localized with SSEA-1 proteins under the observation of confocal microscope. SSEA-1 is a glycoprotein located on the cell membrane[11]. It has been reported that SSEA-1 proteins can be internalized and interacted with LAMP-1 (a lysosome marker) in cytoplasm[48]. We suggest that SSEA-1 may interact with FND to be internalized into the cytoplasm of ECS cells. However, the existence of FNDs in the RA-induced differentiated neuron cells did not alter the expression of β-III-tubulin. These findings demonstrate that ND is a biocompatible nanomaterial for the labeling of neuronal differentiation and neuron cells.

FNDs have excellent photostability in the near-infrared window[24]. FNDs contain more nitrogen-vacancy centers by irradiation damage, and the nitrogen-vacancy centers can emit bright red fluorescence without photobleaching[25]. The fluorescence of injected FNDs stays

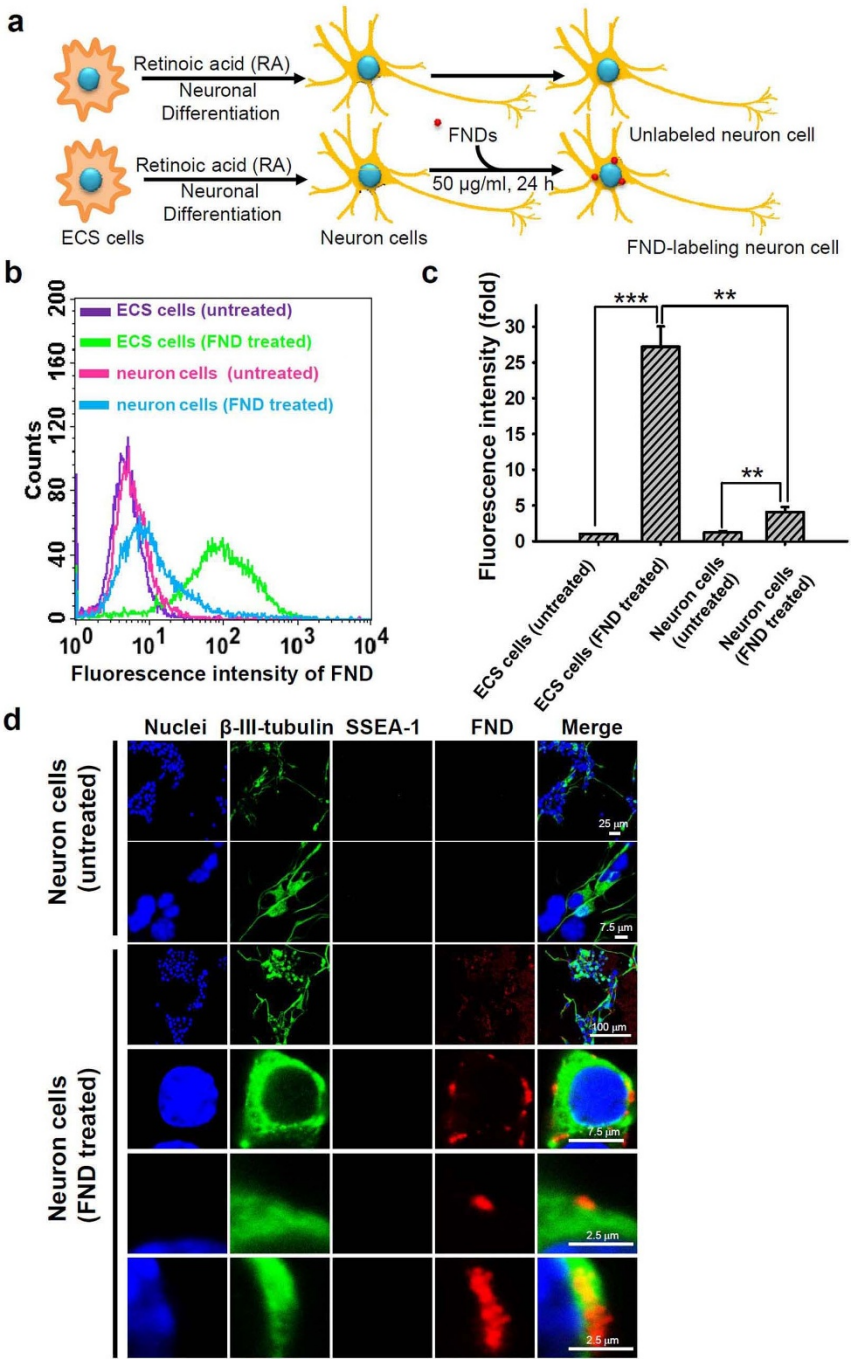

Figure 8 | The labeling and tracking of differentiated neuron cells using FNDs. (a) A model of differentiated neuron cells labeled with FNDs. (b) P19 cells and neuron cells were treated with or without FNDs (50 μg/ml for 24 h). The fluorescence intensity of FNDs in P19 cells and neuron cells were measured by flow cytometer. The fluorescence intensity of FNDs was excited with wavelength 488 nm, and the emission was collected in > 650 nm signal range (FL3-H). (c) The fluorescence intensity of FNDs was quantified from a minimum of 10,000 cells by CellQuest software. Results were obtained from three separate experiments and the bar represented the mean ± S.E. $^{**}p < 0.01$ indicates significant difference between the ECS cells and neuron cells by treatment with FND, or the neuron cells treated with or without FNDs. $^{***}p < 0.001$ indicates significant difference between the untreated and FND-treated ECS cells. (d) P19 cells were differentiated into neuron cells by RA induction. Then the neuron cells were treated with FNDs (50 μg/ml for 24 h). At the end of treatment, the cells were incubated with mouse anti-SSEA-1 and rabbit anti-β-III-tubulin antibodies, and then incubated with goat anti-mouse IgG Cy3 and goat anti-rabbit IgG HiLyte Fluor 488 antibodies. The nuclei were incubated with Hoechst 33258. The red fluorescence intensity of FNDs was excited with wavelength 580 nm, and the emission was collected in 600–700 nm. The blue fluorescence intensity of nuclei was excited with 405 nm and the emission was collected in 415–485 nm. The green fluorescence intensity of β-III-tubulin was excited with 488 nm, and the emission was collected in 505–545 nm. The fluorescence intensity of SSEA-1 was excited with 543 nm, and the emission was collected in 560–580 nm.

for at least one month *in vivo*[38]. We found that FNDs can be tracking after long-term cell culture of 7 days in the differentiated neuron cells using confocal microscope or flow cytometer. Previously, we have shown that the ND-bearing cells can be separated by flow cytometer or magnetic device[34]. The excellent properties indicate that FNDs enable to apply for the labeling and tracking of neuronal differentiation and neuron cells and may be providing potential therapeutics in neural diseases.

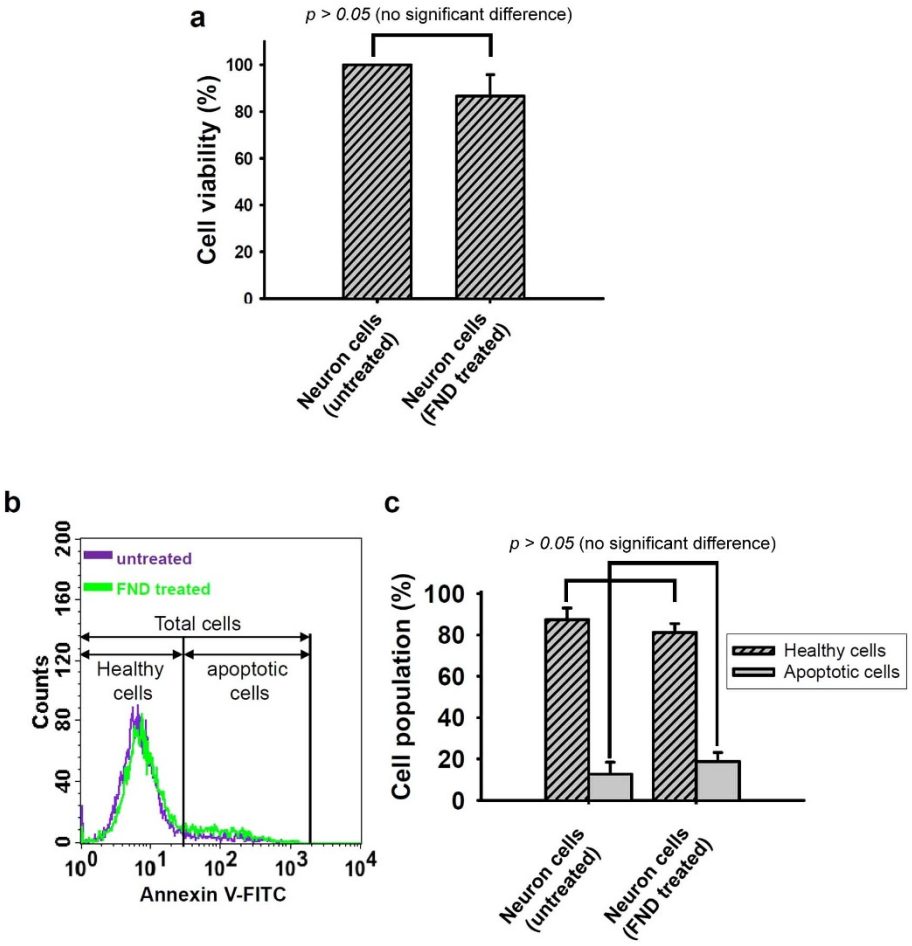

Figure 9 | FNDs do not induce cytotoxicity and apoptosis in the differentiated neuron cells. (a) P19 cells were differentiated into neuron cells. The neuron cells were plated at a density of 7×10^4 cells per well in 24-well plate for 16–20 h. Then the cells were treated with or without FNDs (50 μg/ml for 24 h). At the end of treatment, the cell viability was measured by MTT assays. Results were obtained from three separate experiments and the bar represented the mean ± S.E. (b) P19 cells were differentiated into neuron cells by RA induction. Then the neuron cells were treated with or without FNDs (50 μg/ml for 24 h). The effect of apoptosis was determined by Annexin V-FITC staining using flow cytometer analysis. The populations of Annexin V^+ cells represented cells undergoing apoptosis. (c) The populations of healthy and apoptotic cells were quantified from a minimum of 10,000 cells using CellQuest software. Results were obtained from three separate experiments and the bar represented the mean ± S.E. The percentages of healthy and apoptotic cell populations were not significantly altered by treatment with FNDs ($p > 0.05$).

In summary, we provide the novel insight that FND can be used for the labeling of neuronal differentiation and neuron cells to track cellular localization and distribution. The fluorescence of FNDs in embryonic stem cells, differentiated cells, and neuron cells can be detected by flow cytometer and confocal microscope. The existence of FNDs does not disturb the functions of neuronal differentiation and neuron cells. FND can be utilized for the labeling and tracking of neuronal differentiation and neuron cells derived from stem cells.

Methods

Chemicals and reagents. Hoechst 33258, poly-L-Lysine (PLL), D-Glucose, retinoic acid (RA), and 3-(4,5-dimethyl-thiazol-2-yl)-2,5-diphenyl tetrazolium bromide (MTT) were purchased from Sigma-Aldrich (St. Louis, MO). Laminin, N-2 supplement, SuperScript™ III reverse transcriptase, and oligo-dT 12-18 primer were purchased from Invitrogen (Carlsbad, UA). Sodium pyruvate was purchased from Gibco of Life Technologies (Grand Island, NY). L-glutamine was purchased from Biowest (France).

Antibodies. Anti-stage-specific embryonic antigen-1 (SSEA-1) and horseradish peroxidase (HRP)-conjugated goat anti-mouse IgG antibodies were purchased from GeneTex Inc. (Irvine, CA). Anti-actin antibody was purchased from Millipore (Billerica, MA). Anti-β-III-tubulin antibody was purchased from Cell signaling technology Inc. (Danvers, MA). Anti-rabbit HiLyte Fluor 488-labeld antibody was purchased from AnaSpec (Fremont, CA). Anti-mouse IgG Cy3 antibody was purchased from Jackson ImmunoResearch Laboratories Inc. (West Grove, PA).

Preparation and characterization of fluorescent nanodiamond (FND). Raw ND powders were purchased from Element Six (Ireland). ND powders were radiation-damaged by using either a 40-keV He^+ beam at a dose of $\sim 1 \times 10^{14}$ ions/cm^2 or a 3-MeV H^+ beam at a dose of $\sim 1 \times 10^{16}$ ions/cm^2 to create the optimum amount of vacancies in the diamond crystal lattice, as previously described[24,25]. ND particles were subsequently annealed in vacuum at 800°C for 2 h to form fluorescent ND (FND). After being oxidized in air at 450°C for 1 h, the nanoparticles were washed with concentrated sulfuric and nitric acid (3 : 1, v/v) solution at 100°C for 3 h. The nitrogen-vacancy-containing particles were extensively rinsed in distilled deionized water and stored at room temperature prior to use. The average size of FNDs was ~120 nm that was analyzed by dynamic light scattering (DLS) (please see the Supplementary Figure S2). The particle size and morphological evaluation of FND particles were further observed by a scanning electron microscope (SEM) (please see the Supplementary Figure S3). FNDs carried with negative charge (−23 mV) that was determined by zeta potential analysis. The FTIR spectrum showed FND peak at 1780 cm^{-1}, which indicated the carboxylation group (–COOH) on the surface of FNDs[49].

ECS cell lines and cell culture. P19 was a pluripotent embryonal carcinoma stem (ECS) cell line derived from a teratocarcinoma of C3H/He mice. NT2/D1 cells were derived from human pluripotent ECS cells. P19 cells were maintained in MEM medium (11095, Gibco of Life Technologies, Grand Island, NY). NT2/D1 cells maintained in DMEM medium (12800, Gibco of Life Technologies) The complete medium of MEM contained 10% fetal bovine serum (FBS), 100 unit/ml penicillin, 100 μg/ml streptomycin, and 1 mM sodium pyruvate. The complete medium of DMEM contained 10% FBS, 100 unit/ml penicillin, and 100 μg/ml streptomycin These cells were incubated at 37°C and 5% CO_2 in a humidified incubator (310/ Thermo, Forma Scientific, Inc., Marietta, OH).

Neuronal differentiation of ECS cells. The protocol of neuronal differentiation in ECS cells included three processes: retinoic acid (RA) induction, dissociation of embryoid bodies and neuritogenesis (please see the Supplementary Figure S4). P19 cells were plated at a density of 1×10^6 cells into 100-mm bacterial grade Petri dish in differentiation MEM medium consisting of 5% FBS and 0.5 μM RA, and cultured at 37°C and 5% CO_2 for 4 days to encourage embryoid bodies formation. Two days later, the medium would be refreshed. The fresh medium contained the same concentration of RA. At Day 4, the embryoid bodies were dissociated by trypsinization. The embryoid bodies were collected to 15-ml tube and then incubated for 10 min. After 10 min, removed the suspension and washed the embryoid bodies in pellets by serum-free MEM medium. The embryoid bodies were re-suspended in 2 ml trypsin plus 50 μg/ml DNase I. Then incubated and shaked the tubes every 2 min 37 C for 10 min. Added 8 ml 10% FBS medium to neutralize the trypsin and centrifuged the cells at 100 g for 5 min. After removed the supernatant, re-suspended the cell in serum-free N2.1 medium (MEM medium supplemented with 1x N-2 supplement, 2 mM L-glutamine, 1 mM sodium pyruvate, 0.6% D-Glucose) and counted for re-plating on dishes previously coated with PLL and laminin in N2.1 medium.

MTT assays. The ECS cells were plated in 96-well plates at a density 1×10^4 cells per well, and the neuron cells were plated in 24-well plates at a density 7×10^4 cells per well for 16–20 h. The cells were treated with or without FND (0.1–50 μg/ml for 24 h) in complete medium. Subsequently, the medium was replaced and the cells were incubated with 0.5 mg/ml of 3-(4,5-dimethyl-thiazol-2-yl)-2,5-diphenyl tetrazolium bromide (MTT) in complete medium for 4 h. The surviving cells converted MTT to formazan, which generated a blue-purple color when dissolved in dimethyl sulfoxide (DMSO). The intensity of formazan was measured at 565 nm using a plate reader (VERSAmax, Molecular Dynamics Inc., CA) for enzyme-linked immunosorbent assays. The cell viability was calculated by dividing the absorbance of treated cells by that of the control in each experiment.

Cell growth assays. P19 cells or NT2/D1 cells were plated at a density of 1×10^6 cells per 100-mm Petri dish in complete medium for 24 h. Then the cells were treated with or without FNDs (50 μg/ml for 24 h). After treatment with FND particles, the cells were re-cultured in fresh medium for counting total cell number by every 2 days until total 6 days.

Annexin V-FITC staining. ECS cells were plated at a density of 7×10^5 (P19) or 4×10^5 (NT2/D1) cells per 60-mm Petri dish in complete medium for 16–20 h. Differentiated neuron cells were plated at a density of 1×10^6 cells per 60-mm Petri dish in N2.1 medium for 16–20 h. Thereafter, the cells were treated with or without FNDs (0.1–50 μg/ml for 24 h). Apoptotic cells were stained with an Annexin V-Fluorescein isothiocyanate (FITC) by Apoptosis Detection Kit (BioVision, Mountain View, CA) according to the manufacturer's instructions. Briefly, the cells were collected and responded in 500 μl of binding buffer and 5 μl of Annexin V-FITC reagent. To avoid cell aggregation, the cell suspension was filtered through a nylon mesh membrane. Finally, the samples were analyzed by flow cytometry (FACSCalibur, BectoneDickinson, San Jose, CA). The fluorescence of Annexin V-FITC was excited at a wavelength of 488 nm, and was collected in the green light signal range. The fluorescence intensity was quantified using a minimum of 10,000 cells by CellQuest software (BD Biosciences).

Detection of fluorescence intensity of FND in cells by flow cytometry. P19 and NT2/D1 cells were plated at a density of 7×10^5 and 4×10^5 cells per 60-mm Petri dish, respectively, in complete medium for 16–20 h. Differentiated neuron cells were plated at a density of 1×10^6 cells per 60-mm Petri dish in N2.1 medium for 16–20 h. After treatment with or without FND (0.1–50 μg/ml) for 24 h, the cells were washed twice with PBS. The cells were trypsinized and collected by centrifugation at 1500 rpm for 5 min, and fixed with 75% alcohol at −20°C overnight. Thereafter, the cells were collected by centrifugation at 1500 rpm for 5 min. Then the cell pellets were re-suspended in PBS. To avoid cell aggregation, the cell suspension was filtered through a nylon mesh membrane. Finally, the samples were analyzed by flow cytometry (FACSCalibur, Becton-Dickinson, San Jose, CA). The fluorescence of FNDs was excited at a wavelength of 488 nm, and the emission was collected by > 650 nm signal range (FL3-H). The fluorescence intensity was quantified using a minimum of 10,000 cells by CellQuest software (BD Biosciences).

Western blot. At the end of treatment, the cells were lysed in the ice-cold whole cell extract buffer (pH7.4) containing 250 mM NaCl, 50 mM HEPES, and 0.1% NP-40. The protease inhibitors including 1 μg/ml aprotinin, 0.5 μg/ml leupeptin, and 100 μg/ml 4-(2-aminoethyl) benzenesulfonyl fluoride were added to the cell suspension. The lysate was vibrated for 30 min at 4°C and centrifuged at 12,000 rpm for 10 min. The protein concentrations were determined by the BCA protein assay kit (Pierce, Rockford, IL). Total protein extracts were prepared for western blot analysis using specific SSEA-1 and actin antibodies. Briefly, equal amounts of proteins in samples were subjected to electrophoresis using 10% sodium dodecyl sulfate-polyacrylamide gels. After electrophoretic transfer of proteins onto polyvinylidene fluoride membranes, they were sequentially hybridized with primary antibody and followed with a HRP-conjugated second antibody. Finally, the protein bands were visualized followed by detection with a chemiluminescence kit (PerkinElmer Life and Analytical Sciences, Boston, MA). To verify equal protein loading and transfer, actin was used as the protein loading control. The gel digitizing software, Un-Scan It gel (Ver.6.1, SilkScientific, Inc., Orem, UT), was used to analyze the intensity of bands in X-ray film.

Immunofluorescence staining and confocal microscope. The cells were cultured on coverslips, which were kept in a 35-mm Petri dish for 16–20 h before treatment. After treatment with or without FND (50 μg/ml for 24 h), the cells were washed with isotonic PBS (pH 7.4), and then were fixed with 4% paraformaldehyde solution in PBS for 1 h at 37°C. The coverslips were washed three times with PBS, and non-specific binding sites were blocked in PBS containing 10% FBS, 0.3% Triton X-100 for 1 h. The cells were incubated with mouse anti-SSEA-1 (1 : 100) and rabbit anti-β-III-tubulin antibodies (1 : 100) in PBS containing 10% FBS for overnight at 4°C. Thereafter, the cells were washed three times with 0.3% Triton X-100 in PBS. Subsequently, the cells were incubated with goat anti-mouse Cy3 (1 : 100) and anti-rabbit Hylite 488 (1 : 100) in PBS containing 10% FBS for 1 h at 37°C in dark. The nuclei or chromosomes were stained with Hoechst 33258. After staining, the samples were examined under a Multiphoton Confocal Microscope System (TCS-SP5-X AOBS, Leica, Germany).

Reverse transcription-polymerase chain reaction (RT-PCR). Total cellular RNA was purified by ZR RNA Miniprep (ZYMO research, Irvine, CA) according to the manufacturer's protocol. RNA concentrations were determined by spectrophotometry (Eppendorf, Humburg, Germany). cDNAs were synthesized by SuperScript™ III oligo reverse transcriptase with oligo-dT 12-18 primer. Each reverse transcript was amplified with actin as an internal control. The following primer pairs were used for amplification: β-III-tubulin: 5′-CTGGAGCGCATCAGCGTATAC-3′ and 5′-ATCTGCTGCGTGAGCTCAGG-3; Actin: 5′-TGTATTCCCCTCCATC-GTGG-3′ and 5′-CTCTTTGATGTCACGCACGA TTTC-3′. RT-PCR was performed by a DNA thermal cycler, 5331/Mastercycler gradient (Eppendorf, Hamburg, Germany). The initial denaturation was performed at 95°C for 5 min, followed by 20 cycles at 95°C for 1 min, 56°C, for 1 min, and 72°C for 1 min; and 72°C for 6 min. The PCR products were visualized on 1.5% agarose gels with novel juice staining under UV transillumination, and photograph was taken by a camera (DH27-S3, Medclub, Taoyuan, Taiwan). To verify equal cDNA loading and transfer, actin was used as the protein loading control. The gel digitizing software, Un-Scan-It gel (Ver.6.1, SilkScientific, Inc., Orem, UT), was used to analyze the intensity of bands.

Analysis of β-III-tubulin protein levels by flow cytometry. At the end of treatment, the cells were washed twice with PBS. Then the cells were trypsinized and collected by centrifugation at 1500 rpm for 5 min, and fixed with 75% alcohol at −20°C overnight. Subsequently, non-specific binding sites were blocked in PBS containing 10% FBS, 0.3% Triton X-100 for 1 h. The cells were incubated with rabbit anti-β-III-tubulin antibody (TUJ1, 1 : 100) in PBS containing 10% FBS for overnight at 4°C. Thereafter, the cells were washed three times with 0.3% Triton X-100 in PBS. Subsequently, the cells were incubated with goat anti-rabbit HiLyte Fluor 488-labeled antibody (1 : 100) in PBS containing 10% FBS for 2 h at 37°C in dark. Thereafter, the cells were collected by centrifugation at 1500 rpm for 5 min. Then the cell pellets were re-suspended in PBS. To avoid cell aggregation, the cell suspension was filtered through a nylon mesh membrane. Finally, the samples were analyzed by flow cytometry (FACSCalibur, BectoneDickinson, San Jose, CA). The fluorescence of HiLyte Fluor 488 was excited at a wavelength of 488 nm, and was collected in the green light signal range. The fluorescence intensity was quantified using a minimum of 10,000 cells by CellQuest software (BD Biosciences).

Statistic analysis. Each experiment was repeated at least three times. Data was analyzed using Student's t test or analysis of variance (a comparison of multiple groups), and a p value < 0.05 was considered as statistically significant in all experiments.

1. Brignier, A. C. & Gewirtz, A. M. Embryonic and adult stem cell therapy. *J Allergy Clin Immunol* **125**, S336–S344 (2010).
2. Ding, S. & Schultz, P. G. A role for chemistry in stem cell biology. *Nature Biotechnol* **22**, 833–840 (2004).
3. Evans, M. J. & Kaufman, M. H. Establishment in culture of pluripotential cells from mouse embryos. *Nature* **292**, 154–156 (1981).
4. Martin, G. R. Isolation of a pluripotent cell line from early mouse embryos cultured in medium conditioned by teratocarcinoma stem cells. *Proc Natl Acad Sci U S A* **78**, 7634–7638 (1981).
5. Matin, M. M. *et al.* Specific knockdown of Oct4 and beta 2-microglobulin expression by RNA interference in human embryonic stem cells and embryonic carcinoma cells. *Stem Cells* **22**, 659–668 (2004).
6. Boyer, L. A. *et al.* Core transcriptional regulatory circuitry in human embryonic stem cells. *Cell* **122**, 947–956 (2005).
7. Greber, B., Lehrach, H. & Adjaye, J. Silencing of core transcription factors in human EC cells highlights the importance of autocrine FGF signaling for self-renewal. *BMC Dev Biol* **7** (2007).
8. Andrews, P. W. *et al.* Embryonic stem (ES) cells and embryonal carcinoma (EC) cells: Opposite sides of the same coin. *Biochem Soc Trans* **33**, 1526–1530 (2005).
9. Takahashi, K. & Yamanaka, S. Induction of pluripotent stem cells from mouse embryonic and adult fibroblast cultures by defined factors. *Cell* **126**, 663–676 (2006).
10. Park, I.-H., Lerou, P. H., Zhao, R., Huo, H. & Daley, G. Q. Generation of human-induced pluripotent stem cells. *Nature Protoc* **3**, 1180–1186 (2008).
11. Solter, D. & Knowles, B. B. Monoclonal antibody defining a stage-specific mouse embryonic antigen (SSEA-1). *Proc Natl Acad Sci U S A* **75**, 5565–5569 (1978).

12. Andrews, P. W. *et al.* Comparative analysis of cell surface antigens expressed by cell lines derived from human germ cell tumours. *Int J Cancer* **66**, 806–816 (1996).
13. Przyborski, S. A., Christie, V. B., Hayman, M. W., Stewart, R. & Horrocks, G. M. Human embryonal carcinoma stem cells: models of embryonic development in humans. *Stem Cells Dev* **13**, 400–8 (2004).
14. McBurney, M. W., Jonesvilleneuve, E. M. V., Edwards, M. K. S. & Anderson, P. J. Control of muscle and neuronal differentiation in a cultured embryonal carcinoma cell line. *Nature* **299**, 165–167 (1982).
15. Soprano, D. R., Teets, B. W. & Soprano, K. J. Role of retinoic acid in the differentiation of embryonal carcinoma and embryonic stem cells. in *Vitamin A,* Vol. 75 (ed. Litwack, G) 69–95 (2007).
16. van der Heyden, M. A. G. & Defize, L. H. K. Twenty one years of P19 cells: what an embryonal carcinoma cell line taught us about cardiomyocyte differentiation. *Cardiovasc Res* **58**, 292–302 (2003).
17. Kim, J. H. *et al.* Dopamine neurons derived from embryonic stem cells function in an animal model of Parkinson's disease. *Nature* **418**, 50–56 (2002).
18. Lindvall, O. & Kokaia, Z. Stem cells for the treatment of neurological disorders. *Nature* **441**, 1094–1096 (2006).
19. Glat, M. J. & Offen, D. Cell and Gene Therapy in Alzheimer's Disease. *Stem Cells Dev* **22**, 1490–1496 (2013).
20. Behrstock, S. *et al.* Human neural progenitors deliver glial cell line-derived neurotrophic factor to parkinsonian rodents and aged primates. *Gene Ther* **13**, 379–388 (2006).
21. Dauer, W. & Przedborski, S. Parkinson's disease: Mechanisms and models. *Neuron* **39**, 889–909 (2003).
22. Wang, F. *et al.* GDNF-pretreatment enhances the survival of neural stem cells following transplantation in a rat model of Parkinson's disease. *Neurosci Res* **71**, 92–98 (2011).
23. Mochalin, V. N., Shenderova, O., Ho, D. & Gogotsi, Y. The properties and applications of nanodiamonds. *Nat Nanotechnol* **7**, 11–23 (2012).
24. Yu, S. J., Kang, M. W., Chang, H. C., Chen, K. M. & Yu, Y. C. Bright fluorescent nanodiamonds: no photobleaching and low cytotoxicity. *J Am Chem Soc* **127**, 17604–5 (2005).
25. Chang, Y. R. *et al.* Mass production and dynamic imaging of fluorescent nanodiamonds. *Nat Nanotechnol* **3**, 284–8 (2008).
26. Chao, J. I. *et al.* Nanometer-sized diamond particle as a probe for biolabeling. *Biophys J* **93**, 2199–208 (2007).
27. Chang, I. P., Hwang, K. C. & Chiang, C. S. Preparation of fluorescent magnetic nanodiamonds and cellular imaging. *J Am Chem Soc* **130**, 15476–81 (2008).
28. Liu, K. K. *et al.* Alpha-bungarotoxin binding to target cell in a developing visual system by carboxylated nanodiamond. *Nanotechnology* **19**, 205102 (2008).
29. Liu, K. K. *et al.* Covalent linkage of nanodiamond-paclitaxel for drug delivery and cancer therapy. *Nanotechnology* **21**, 315106 (2010).
30. Edgington, R. J. *et al.* Patterned neuronal networks using nanodiamonds and the effect of varying nanodiamond properties on neuronal adhesion and outgrowth. *J Neural Eng* **10**, 056022 (2013).
31. Le, X. L. *et al.* Fluorescent diamond nanoparticle as a probe of intracellular traffic in primary neurons in culture. *Colloidal Nanocrystals for Biomedical Applications VII Book Series: Proc of SPIE* **8232**, 823203 (2012).
32. Liu, K. K., Cheng, C. L., Chang, C. C. & Chao, J. I. Biocompatible and detectable carboxylated nanodiamond on human cell. *Nanotechnology* **18**, 325102 (2007).
33. Liu, K. K., Wang, C. C., Cheng, C. L. & Chao, J. I. Endocytic carboxylated nanodiamond for the labeling and tracking of cell division and differentiation in cancer and stem cells. *Biomaterials* **30**, 4249–59 (2009).
34. Lien, Z. Y. *et al.* Cancer cell labeling and tracking using fluorescent and magnetic nanodiamond. *Biomaterials* **33**, 6172–85 (2012).
35. Schrand, A. M., Lin, J. B., Hens, S. C. & Hussain, S. M. Temporal and mechanistic tracking of cellular uptake dynamics with novel surface fluorophore-bound nanodiamonds. *Nanoscale* **3**, 435–45 (2011).
36. Vaijayanthimala, V., Tzeng, Y. K., Chang, H. C. & Li, C. L. The biocompatibility of fluorescent nanodiamonds and their mechanism of cellular uptake. *Nanotechnology* **20**, 425103 (2009).
37. Paget, V. S. *et al.* Carboxylated nanodiamonds are neither cytotoxic nor genotoxic on liver, kidney, intestine and lung human cell lines. *Nanotoxicology* DOI:10.3109/17435390.2013.855828 (2013).
38. Vaijayanthimala, V. *et al.* The long-term stability and biocompatibility of fluorescent nanodiamond as an in vivo contrast agent. *Biomaterials* **33**, 7794–802 (2012).
39. Chow, E. K. *et al.* Nanodiamond therapeutic delivery agents mediate enhanced chemoresistant tumor treatment. *Sci Transl Med* **3**, 73ra21 (2011).
40. Blaber, S. P. *et al.* Effect of labeling with iron oxide particles or nanodiamonds on the functionality of adipose-derived mesenchymal stem cells. *PLoS One* **8**, e52997 (2013).
41. Wu, T. J. *et al.* Tracking the engraftment and regenerative capabilities of transplanted lung stem cells using fluorescent nanodiamonds. *Nat Nanotechnol* **8**, 682–689 (2013).
42. Power, C. & Rasko, J. E. J. Promises and challenges of stem cell research for regenerative medicine. *Ann Intern Med* **155**, 706–713 (2011).
43. Jonesvilleneuve, E. M. V., Rudnicki, M. A., Harris, J. F. & McBurney, M. W. Retinoic acid-induced neural differentiation of embryonal carcinoma cells. *Mol Cell Biol* **3**, 2271–2279 (1983).
44. Duester, G. Retinoic acid synthesis and signaling during early organogenesis. *Cell* **134**, 921–931 (2008).
45. Memberg, S. P. & Hall, A. K. Dividing neuron precursors express neuron-specific tubulin. *J Neurobiol* **27**, 26–43 (1995).
46. Maia, J. *et al.* Controlling the neuronal differentiation of stem cells by the intracellular delivery of retinoic acid-loaded nanoparticles. *ACS Nano* **5**, 97–106 (2011).
47. Santos, T. *et al.* Polymeric nanoparticles to control the differentiation of neural stem cells in the subventricular one of the brain. *ACS Nano* **6**, 10463–10474 (2012).
48. Yagi, H., Yanagisawa, M., Kato, K. & Yu, R. K. Lysosome-associated membrane protein 1 is a major SSEA-1-carrier protein in mouse neural stem cells. *Glycobiology* **20**, 976–981 (2010).
49. Chu, Z. *et al.* Unambiguous observation of shape effects on cellular fate of nanoparticles. *Sci Rep* **4**, 4495 (2014).

Acknowledgments

This work was supported by the grants from the National Science Council (NSC 99-2311-B-009-003-MY3), National Chiao Tung University (103W970), and Veterans General Hospitals University System of Taiwan Joint Research Program (VGHUST103-G5-4-3). The authors also thank the core facility of Multiphoton and Confocal Microscope System (MCMS) in National Chiao University, Hsinchu, Taiwan.

Author contributions

T.-C.H. and K.-K.L. conducted experiments, H.-C.C., E.H. and J.-I.C. supplied materials and equipments, T.-C.H., K.-K.L. and J.-I.C. designed experiments and wrote the manuscript. All authors discussed on the manuscript.

Additional information

Supplementary information accompanies this paper at http://www.nature.com/scientificreports

Competing financial interests: The authors declare no competing financial interests.

How to cite this article: Hsu, T.-C., Liu, K.-K., Chang, H.-C., Hwang, E. & Chao, J.-I. Labeling of neuronal differentiation and neuron cells with biocompatible fluorescent nanodiamonds. *Sci. Rep.* **4**, 5004; DOI:10.1038/srep05004 (2014).